Title
Land-atmosphere coupling and climate prediction over the U.S. Southern Great Plains

Journal
Journal of Geophysical Research: Atmospheres, 121(20)

ISSN
2169-897X

Authors
Williams, Ian N
Lu, Yaqiong
Kueppers, Lara M
et al.

Publication Date
2016-10-27

DOI
10.1002/2016jd025223

Peer reviewed

Land-atmosphere coupling and climate prediction over the U.S. Southern Great Plains

Ian N. Williams

Yaqiong Lu

Lara M. Kueppers

William J. Riley

Sebastien C. Biraud

Justin E. Bagley
Margaret S. Torn
First published: 05 October 2016
https://doi.org/10.1002/2016JD025223
Cited by: 7
UC-eLinks

Abstract

Biases in land-atmosphere coupling in climate models can contribute to climate prediction biases, but land models are rarely evaluated in the context of this coupling. We tested land-atmosphere coupling and explored effects of land surface parameterizations on climate prediction in a single-column version of the National Center for Atmospheric Research Community Earth System Model (CESM1.2.2) and an off-line Community Land Model (CLM4.5). The correlation between leaf area index (LAI) and surface evaporative fraction (ratio of latent to total turbulent heat flux) was substantially underpredicted compared to observations in the U.S. Southern Great Plains, while the correlation between soil moisture and evaporative fraction was overpredicted by CLM4.5. To estimate the impacts of these errors on climate prediction, we modified CLM4.5 by prescribing observed LAI, increasing soil resistance to evaporation, increasing minimum stomatal conductance, and increasing leaf reflectance. The modifications improved the predicted soil moisture-evaporative fraction (EF) and LAI-EF correlations in off-line CLM4.5 and reduced the root-mean-square error in summer 2 m air temperature and precipitation in the coupled model. The modifications had the largest effect on prediction during a drought in summer 2006, when a warm bias in daytime 2 m air temperature was reduced from +6°C to a smaller cold bias of −1.3°C, and a corresponding dry bias in precipitation was reduced from −111 mm to −23 mm. The role of vegetation in droughts and heat waves is underpredicted in CESM1.2.2, and improvements in land surface models can improve prediction of climate extremes.

1 Introduction

The land surface is coupled to the atmosphere through water, energy, and carbon fluxes. As a consequence of this coupling, poor representation of land surface processes can contribute to

prediction biases in weather and climate models [*Viterbo and Beljaars*, 1995; *Beljaars et al.*, 1996; *Xue et al.*, 1996, 2010; *Lawrence et al.*, 2007]. Many modeling studies have shown that soil moisture can influence climate prediction [*Shukla and Mintz*, 1982; *Beljaars et al.*, 1996; *Koster et al.*, 2006, 2010; *Guo et al.*, 2011]. However, different climate models have markedly different relationships between soil moisture and surface latent heat flux [*Dirmeyer et al.*, 2006; *Guo et al.*, 2006], as revealed by the Global Land-Atmosphere Coupling Experiment (GLACE) [*Koster et al.*, 2006]. A related problem is the tendency for land models used in climate prediction to systematically overestimate the degree of coupling between soil moisture and surface energy partitioning when compared to observations [*Dirmeyer et al.*, 2006; *Guo et al.*, 2006; *Ferguson et al.*, 2012]. Furthermore, climate models with less evapotranspiration tend to have a summer warm bias over the central U.S., suggesting a role of land-atmosphere feedbacks in climate prediction biases [*Merrifield and Xie*, 2016]. Similarly, uncertainties in these feedbacks contribute to future climate projection uncertainties at regional scales [*Cheruy et al.*, 2014].

Past studies of land-atmosphere coupling have focused on soil moisture states as a measure of land surface state, since there is a well-known reduction in evapotranspiration (hereafter ET) due to soil moisture stress as soil moisture declines past a threshold [e.g., *Seneviratne et al.*, 2010]. In wet soil conditions, ET may be limited by available energy [e.g., *Ford et al.*, 2014]. However, it is also recognized that vegetation plays an important role in surface water and energy balance [*Wilson et al.*, 2002; *Gentine et al.*, 2007; *Williams et al.*, 2012]. Observations indicate that vegetation state is strongly correlated with surface energy partitioning in several ecosystems, suggesting that vegetation plays an important role in land-atmosphere coupling [*Williams and Torn*, 2015]. When soil moisture is not a limiting factor, transpiration is governed by biogeochemical controls on canopy photosynthesis, as well as wind speed, vapor pressure deficit, and net radiation [e.g., *Sellers et al.*, 1996]. The soil moisture limitation on ET in vegetated regions is determined by plant responses to soil drying [e.g., *Siqueira et al.*, 2008]. Thus, both soil moisture and vegetation state are important in characterizing the influence of the land surface on surface energy partitioning.

One objective of this study is to evaluate modeled land-atmosphere coupling using both soil moisture and vegetation metrics. Furthermore, while it is well known that land models inaccurately represent some of the mechanisms linking soil, vegetation, and surface energy partitioning [*Tang and Riley*, 2013; *Swenson and Lawrence*, 2014], it is less clear how these deficiencies relate to climate prediction. An additional objective of this study is to estimate the impact that correcting for such deficiencies would have on improving prediction in current

climate models. By using observationally based metrics of land-atmosphere coupling, our approach differs from past studies [e.g., *Lawrence et al.*, 2007] that used flux observations in evaluating and exploring impacts of land model errors on climate prediction.

Land-atmosphere coupling can be divided into a terrestrial segment that includes the effects of soil moisture and vegetation state on surface energy balance, and an atmospheric segment that includes the effects of surface energy balance on the atmospheric planetary boundary layer (PBL), clouds, and precipitation [*Dirmeyer*, 2011; *Guo et al.*, 2011]. Surface energy balance can be characterized by net radiation and its partitioning into sensible, latent, and ground heat fluxes. A useful measure of the surface energy partitioning between sensible and latent heat fluxes is the evaporative fraction (EF), or fraction of latent relative to total sensible and latent heat flux [*Guo et al.*, 2006; *Santanello et al.*, 2011]. Changes in EF can directly influence precipitation by increasing the column-integrated water vapor and hence the precipitation amount, in a precipitation recycling mechanism [*Brubaker et al.*, 1993]. Changes in EF can also indirectly influence precipitation by deepening the PBL and triggering moist convection [*Eltahir*, 1998; *Schar et al.*, 1999; *Findell and Eltahir*, 2003; *Betts*, 2007; *Berg et al.*, 2013].

The terrestrial branch of land-atmosphere coupling is often quantified by the correlation between upper layer soil moisture and EF, using the Pearson correlation coefficient [*Phillips and Klein*, 2014] or the Kendall rank correlation coefficient [*Ferguson et al.*, 2012]. Based on this metric, previous studies have shown that soil moisture is too strongly coupled to surface energy partitioning in many land models used in climate models [*Ferguson et al.*, 2012]. Such weak observed correlations may indicate that climate models are overestimating the land surface influence on climate variability [*Phillips and Klein*, 2014]. Another possibility to be explored here is that land models are not overestimating the overall coupling but rather are poorly representing important mechanisms of this coupling; specifically, they may be overestimating the role of upper layer soil moisture but underestimating the role of vegetation (and root-zone soil moisture) in surface energy partitioning. The observed correlation between leaf area index (LAI) and EF is a factor of 2–3 times larger than the correlation between soil moisture and EF, using daily data for summer months at several sites including the U.S. Southern Great Plains (SGP) [*Williams and Torn*, 2015]. Thus, the relationship between soil moisture and EF alone may not always be sufficient to characterize the land surface influence on EF.

Here LAI is defined as the one-sided area of green leaves per unit ground area. Transpiration and photosynthesis are coupled, since both water vapor and carbon dioxide are exchanged through the stomata. LAI plays an important role in determining the surface albedo and the amount of light absorbed by the canopy for photosynthesis. Canopy photosynthesis in turn couples LAI and

transpiration [*Sellers et al.*, 1996], since stomatal conductance is a function of photosynthesis as well as CO_2 concentration and relative humidity at the leaf surface. Higher LAI results in a higher canopy photosynthetic rate and transpiration, all else being equal. Additionally, higher LAI can lead to higher transpiration by increasing the surface area for stomatal conductance [e.g., *Wilson and Baldocchi*, 2000]. LAI is also important in determining the interception of precipitation and shading of the soil surface by the leaves, which can reduce soil evaporation.

Climate models are sensitive to the representation of vegetation and its control on surface energy balance [*Xue et al.*, 1996; *Lawrence et al.*, 2007; *Jarlan et al.*, 2008; *Boussetta et al.*, 2013]. Furthermore, transpiration is the dominant component of ET in many climates [*Lawrence et al.*, 2007; *Schlesinger and Jasechko*, 2014], and some land models are known to underestimate the contribution of transpiration to ET [*Lawrence et al.*, 2007]. Living plants maintain hydraulic conductivity of soil water from the root zone to the leaves, whereas soil evaporation can become diffusion limited once the upper soil layer dries [*Tang and Riley*, 2013; *Swenson and Lawrence*, 2014]. Transpiration may therefore be particularly important for ET when root-zone soil moisture is available but upper layer soil moisture is depleted. Additionally, while ET affects the partitioning of net radiation (and ground heat flux) into latent and sensible heat flux, the albedo influences the net radiation itself. Therefore, another role of a land surface model to be explored here is in predicting the surface albedo.

We hypothesize that the representation of land-atmosphere coupling in climate models can affect summer climate prediction. Our objectives are to (1) evaluate modeled land-atmosphere coupling using both soil moisture and vegetation metrics; (2) improve prediction of this coupling within the parameter space of the National Center for Atmospheric Research (NCAR) Community Land Model (CLM4.5), for summer months over the U.S. Southern Great Plains; and (3) use the modified parameters to assess the effects of the improved representation of land-atmosphere coupling on climate prediction in a single-column version of CESM1.2.2.

2 Methods

2.1 Model Description and Domain

We used the NCAR Community Earth System Model version 1.2.2 (hereafter CESM1.2.2), which includes the Community Land Model (CLM4.5) [*Oleson*, 2013] and the Community Atmosphere Model (CAM5) [*Neale et al.*, 2010]. CAM5 has 30 vertical layers and uses the University of Washington moist turbulence (boundary layer) scheme by *Bretherton and Park* [2009]. The grid cell of the single-column model was centered over the U.S. Department of

Energy Atmospheric Radiation Measurement (ARM) Climate Research Facility in the U.S. Southern Great Plains (SGP), hereafter referred to as ARM-SGP. The effective domain size of a single-column model corresponds to that of the forcing data set used to supply the advective tendencies and vertical velocities, which was approximately 4°latitude × 4°longitude (see section 2.2 below for details).

Both off-line CLM4.5 and a (coupled) single-column version of CESM1.2.2 were used in this study. CLM4.5 represents subgrid-scale variability by predicting surface turbulent heat fluxes and albedo for each subgrid-scale plant functional type (PFT), before averaging over all PFTs within each grid cell. All PFTs share the same soil moisture. Following the "tiling" method [*Koster and Suarez*, 1992], there is a separate canopy air space for each PFT, and sensible and latent heat fluxes differ for different PFTs within the same grid cell. The collection of PFTs forms a mosaic of tiles within the grid cell, which are not spatially resolved. The albedo over vegetated surfaces differs for different PFTs and is a function of leaf optical properties and LAI. The coupled model grid cell (described below) has seven PFTs in the grid. The PFTs by percentage cover are C3 crop (35%), C4 grass (18%), and C3 nonarctic grass (27%). The remainder is nonvegetated (8%), needleleaf evergreen trees (4%), broadleaf deciduous trees (7%), and shrubs (1%).

We tested a version of CLM with two separate soil columns for the two dominant vegetation types (C3 and C4 grass and C3 crop) but found little sensitivity to shared versus separate soil columns (result not shown). This may reflect the fact that soil moisture is not typically limiting when winter wheat is grown (October to early June), such that the grass PFT (which has peak LAI in July) may not strongly compete with the crop PFT for the same soil moisture. Additionally, grasses in this region are a mixture of both C3 and C4 species [*Torn et al.*, 2011], and they may share the same soil moisture.

2.2 Single-Column Model Forcing

The single-column CESM1.2.2 was forced with prescribed winds (including vertical velocity) and horizontal advective tendencies obtained from an observational data assimilation product, hereafter referred to as column forcing. The column forcing was derived from a constrained variational analysis that adjusted numerical weather predictions toward surface and top-of-atmosphere measurements while balancing column mass, momentum, heat, and water, over an approximately 4° × 4° domain [*Xie et al.*, 2004]. An advantage of prescribing the large-scale circulation is that the effects of observed weather events can be represented in the single-column model via prescribed advective tendencies and vertical velocity. This approach allowed us to

compare predictions directly to observations for the specific time corresponding to that of the column forcing data set. The role of column forcing is similar to that of lateral boundary conditions specified in a regional climate model, and it similarly reduces model sensitivity to the initial atmospheric condition since the model weather variability is strongly determined by the prescribed forcing as opposed to internal atmospheric dynamics.

2.3 Vegetation Phenology

We used the Satellite Phenology version of CLM4.5, which allows for the LAI to be prescribed from observations, while still representing the leaf-level coupling of CO_2 and H_2O exchanges. The default prescribed phenology version of CLM4.5 has climatological monthly LAI and stem area index (SAI) assigned to each grid cell and PFT. For the off-line runs, CLM4.5 was run as a single point forced with site-level meteorology and (in our nondefault experiments) with daily "real-time" varying LAI and SAI derived from ground-based normalized difference vegetation index (NDVI) measurements for years 2000–2010. The NDVI measurements were collocated with the flux measurements in the crop and pasture fields. This approach avoided the added uncertainty of potential spatial scale mismatches between modeled and observed LAI at the measurement site, as well between the flux and NDVI measurement footprints.

For the coupled single-column CESM experiments, we used monthly LAI derived from the Moderate Resolution Imaging Spectroradiometer (MODIS) data at 250 m resolution, separated into different PFTs and averaged over a 4° × 4°domain surrounding the SGP site. In other words, each 250 m grid cell was assigned a PFT (following the method in *Riley et al.* [2009]) and all MODIS-derived grid cell LAI values were averaged over the domain conditional on PFT, to create a domain-averaged monthly LAI for each PFT. SAI was estimated from LAI following the same method used in CLM4.5 [*Zeng et al.*, 2002]. At the time of this study, gridded MODIS LAI and column forcing data were prepared for the 6 year period from 2003 to 2008, which is the period for which we ran the single-column experiments. Previous studies provide additional information on the ground-based LAI and surface flux measurements at the SGP site [*Williams and Torn*, 2015], and on the MODIS data used in this study [*Riley et al.*, 2009].

2.4 Spin-Up Procedure and Land Model Forcing

In both off-line and coupled simulations, the land surface was spun up to steady state using observed atmospheric forcing [*Qian et al.*, 2006] from 1 January 1980 to 1 January 2000. For the off-line CLM4.5 experiments, we continued the off-line integration from 1 January 2000 to 1 January 2010, using available site-level meteorological data from the Central Facility of the SGP site as atmospheric forcing. For the coupled model land surface initial conditions, we continued

the off-line CLM4.5 integrations from 1 January 2000 to 1 January 2010 using atmospheric forcing from the same variational analysis product [*Xie et al.*, 2004] used for the column forcing over the larger 4° × 4° domain described in section 2.2. The coupled model was initialized with the spun-up land surface and nudged toward the observed atmospheric state for 2 weeks to obtain a land surface state consistent with the atmospheric model physics. The coupled model was then initialized with atmospheric observations at 00:00 UTC on 1 June and was run continuously through 1 September for each year in this study. A similar spin-up and nudging procedure has been used to initialize and evaluate global models using observations [*Phillips et al.*, 2004; *Ma et al.*, 2014]. The results were not sensitive to the initial atmospheric condition, as shown at the end of the results (section 3.2).

2.5 Coupling Metrics

We quantify the terrestrial segment of land-atmosphere coupling using the correlation coefficient [e.g., *Phillips and Klein*, 2014] for the relationships between soil moisture and EF, and between LAI and EF. We also use a so-called sensitivity index, given by the product of the soil moisture standard deviation and the slope of the linear regression of EF on soil moisture [*Dirmeyer*, 2011]. Our definition of terrestrial coupling refers to a one-way influence of the land surface state on the atmosphere and can be distinguished from two-way coupling involving feedbacks [*Seneviratne et al.*, 2010]. More specifically, coupling typically refers to the relationship between the land surface state and atmospheric state variables, while the coupling metrics described here focus on the relationship between land surface state and fluxes at the land-atmosphere interface. These relationships are indicators of the coupling (for example) between soil moisture and 2 m air temperature [*Seneviratne et al.*, 2010].

2.6 Parameterization Sensitivity

Several parameters were investigated to determine if CLM4.5 can be modified to better predict observed land-atmosphere coupling. For prediction of EF and its relation to soil moisture and LAI, we focused on four parameters including minimum stomatal conductance, soil beta factor, litter-layer resistance, and the maximum rate of carboxylation (V_{cmax}). Other parameters that were explored but did not substantially improve simulation of land-atmosphere coupling include parameters related to the soil moisture stress factor btran (soil water potentials at full stomatal closure and full stomatal opening), rooting distribution parameters, and parameters related to soil hydrology (soil texture, soil organic matter density, mean topographic slope, soil color, standard deviation of elevation, soil column depth, and maximum fractional saturated area). These parameters did not substantially change metrics of terrestrial land-atmosphere coupling in terms

of either soil moisture-EF, or LAI-EF correlations at the SGP site. Additionally, leaf reflectance was modified in accordance with observed surface albedo, as described in section 3.1 below.

Of the four parameter changes related to EF, the most critical for land-atmosphere coupling was to increase the minimum stomatal conductance from 10 mmol m^{-2} s^{-1} to 60 mmol m^{-2} s^{-1} for C3 and from 40 mmol m^{-2} s^{-1} to 80 mmol m^{-2} s^{-1} for C4 plants. These higher values are plausible in light of recent direct measurements with diffusion porometers [*Barnard and Bauerle*, 2013] and are similar to but smaller than recently proposed increases in CLMs minimum stomatal conductance for the vegetation types considered here [*Lombardozzi et al.*, 2015]. The slope of the Ball-Berry equation was not changed.

Although the increase in minimum stomatal conductance improved soil moisture-EF and LAI-EF correlations, it also led to higher latent heat flux predictions than observed. Therefore, we also increased the dry litter-layer resistance by a factor of 2, and decreased the soil beta factor by a factor of 2. The soil beta factor attempts to quantify the effect of molecular diffusion within the dry part of the soil on the surface turbulent flux. These changes are consistent with previous results suggesting that CLM4.5 overestimates bare soil evaporation when the uppermost soil layer dries and evaporation becomes limited by diffusion [*Tang and Riley*, 2013; *Swenson and Lawrence*, 2014]. The simpler parameter changes introduced here are for the express purpose of estimating the effects of errors in predicted land-atmosphere coupling on climate prediction.

As a final modification, we decreased the maximum rate of carboxylation (V_{cmax}) by 30% to reduce the predicted maximum EF at high LAI. This change was made to better match observed maximum EF and gross primary productivity (GPP) inferred from observed net ecosystem exchange of CO_2 (GPP result not shown). Although V_{cmax} is constrained by measurements of leaf gas exchange, a single number is assigned to each PFT in CLM4.5 [*Bonan et al.*, 2012]. A 30% change from the default value of V_{cmax} is plausible considering the large spatial and temporal variability in V_{cmax} measurements within a given PFT.

We present the results of all four parameter changes together in one experiment, because the effects of changing V_{cmax} and soil parameters were largely additive to the effects of increasing the minimum stomatal conductance. There was no evidence of interactions between the different parameter changes in this study. Although a more comprehensive parameter sensitivity test could be performed, our focus here is on assessing the potential impact of improved parameterization of the terrestrial segment of land-atmosphere coupling on climate prediction rather than identifying the best parameter values per se. Table (1) gives a description of each of the off-line and coupled model experiments.

Table 1. Names and Descriptions of Experiments

Experiment Name	Description
CLM-default	CLM4.5 with default LAI climatology and site-level meteorology
CLM-LAI	Prescribed LAI from site observations
CLM-LAI-ref	As in CLM-LAI but with modified leaf reflectance
CLM-ref	Modified leaf reflectance only
CLM-LAI-ref-res	As in CLM-LAI-ref but with increased soil resistance and increased minimum stomatal conductance
CESM-default	CAM5 and CLM4.5 with default LAI climatology
CESM-LAI-ref	Prescribed LAI from MODIS and modified leaf reflectance
CESM-ref	Modified leaf reflectance only
CESM-LAI-ref-res	As in CESM-LAI-ref but with increased soil resistance and increased minimum stomatal conductance

2.7 Evaluation Data and Scaling

The site-level observations used in this study are half hourly, including latent and sensible heat flux and radiation measurements in a predominantly winter wheat field (hereafter referred to as the crop site), and in a pasture field consisting of C3 and C4 grasses. Both sites are located in the ARM-SGP domain. The crop and pasture fields are adjacent and experience the same weather (the same atmospheric forcing). These two (unirrigated) sites represent the dominant land use types in the SGP [*Cooley et al.*, 2005; *Riley et al.*, 2009] and correspond to the three dominant PFTs within the CLM grid cell (C3 crops, and C3 and C4 grasses). Our site-level analyses included the warm season defined as 1 May to 1 September for years 2000–2008 at the pasture site, and 1 April to 1 September for years 2003–2010 for the crop site, with the different dates reflecting the availability of data as well as the earlier growing season for the winter wheat planted at the crop site. Results were not sensitive to the exact choice of months in the analyses (within 1–2 months).

The flux measurements were made by eddy correlation and Bowen ratio methods. The eddy covariance instrument was located in the middle of the crop field at a height of 4 m. At this height, the field is within the flux footprint for the prevailing southerly flow in late spring and summer months. Similarly, the energy-balance Bowen ratio measurement was located in a grass field that extends a few hundred meters to the south of the measurement system. We used these site-level flux measurements to evaluate and constrain the land model parameters on a PFT basis. In other words, we compared the average of C3 and C4 grass PFTs in CLM4.5 to flux measurements over the pasture site and compared the C3 crop PFT in CLM4.5 to measurements over the crop site.

The soil moisture measurements were made using electrical capacitance sensors in the crop site, and heat-dissipation sensors in the pasture site. For the crop site, there were four sensors at 10 cm depth, and four sensors at 20 cm depth. For the pasture site, there were two sensors each at depths of 5, 15, 25, 35, 60, and 85 cm. Here we used the average of the 10 cm sensors at the crop site (results were not qualitatively different for the 20 cm sensor) and averaged the 5 and 15 cm sensors at the pasture site. Results from the deeper sensors at the pasture site will be discussed (see section 4).

All model-observation comparisons were made at consistent spatial scales. We ran separate off-line CLM4.5 experiments for the comparison to site-level data, by prescribing site-level LAI observations for the two dominant vegetation types (C3 and C4 grass and C3 crop PFTs). Likewise, we forced the off-line land model with site-level meteorological measurements. To

represent vegetation cover at the climate model grid scale, we ran the single-column model with prescribed 250 m resolution MODIS LAI averaged over a 4° × 4° degree area centered over the ARM-SGP. We compared the single-column model output to an observationally derived estimate of surface fluxes at the same resolution, based on observations from the Oklahoma and Kansas Mesonet stations and from the ARM Climate Research Facility [*Xie et al.*, 2004].

3 Results

3.1 Off-Line Land Model (CLM4.5)

The default prescribed LAI in CLM4.5 lacks distinction between the growing seasons of pasture (C3 and C4 grass) and crop (typically winter wheat, harvested in June) compared to the site-level observations (Figure 1). The default data set has peak LAI occurring in May for both vegetation types (Figure 1a). In contrast, observed crop LAI peaks in April and pasture LAI peaks in June (Figure 1b). Note that the crop site-level LAI does not drop to 0 following harvest, due to weeds and because corn (maize) grew during summer months in two of the years. As shown later, the differences between default CLM prescribed LAI and observed LAI are not specific to this site and also extend across the SGP regionally. The default LAI is a 1 km monthly climatology of MODIS, which is spatially too coarse to distinguish between different fields having different PFTs and does not represent interannual variability in LAI.

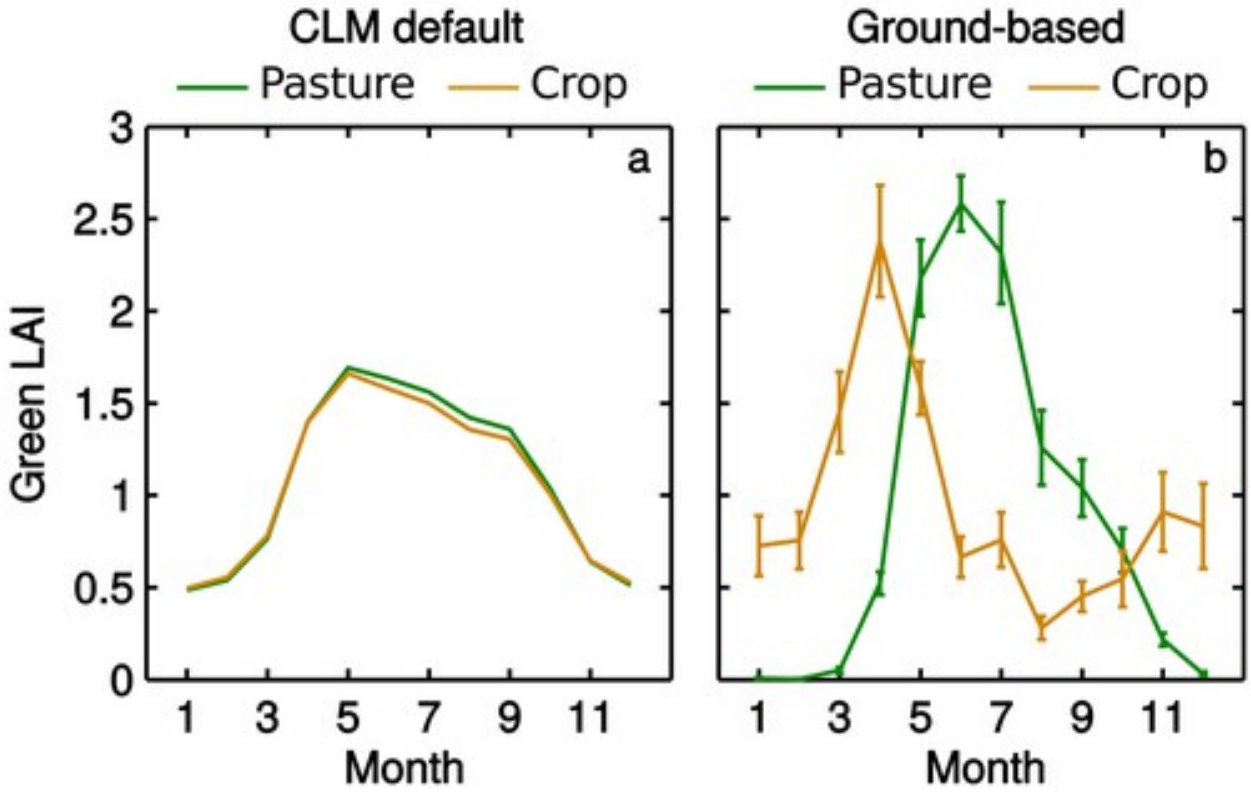

Figure 1

Open in figure viewerPowerPoint

(a) CLM default LAI and (b) ground-based observed LAI separated into pasture (green lines) and crop (orange lines). Each point is a monthly average over multiple years. Error bars indicate standard error of the monthly mean.

Caption

We compared albedo measurements to default CLM (hereafter CLM-default) and CLM with prescribed ground-based LAI measurements (hereafter CLM-LAI). Both the default and modified LAI configurations underestimated the surface albedo by nearly 30% in the summer months for the pasture site (Figures 2a and 2b). To better predict surface albedo at this site, we increased the near-infrared reflectance of green leaves for crop and grass PFTs from a default value of 0.35 to 0.5, in accordance with higher literature values [*Myneni and Ross*, 2012]. The default values vary with PFT, such that a given PFT has the same leaf reflectance across all grid cells [*Oleson*, 2013]. The default visible reflectance was smaller, and also closer to the literature values, and was not changed. The higher leaf reflectance improved albedo prediction for the pasture site (Figure 2c). Likewise, the 40 W m^{-2} bias in upwelling shortwave radiation was reduced to less than 10 W m^{-2} in summer months (Figures 2d–2f). For the crop site, the same increase in leaf reflectance also improved albedo and upwelling shortwave radiation relative to both the default prescribed and observed (site-level) prescribed LAI configurations (Figures 2g–2l). Using the observed LAI yielded a larger improvement in predicted albedo for the crop site relative to the pasture (Figures 2g and 2h), likely due to the substantial overestimation of crop LAI by default CLM in summer months.

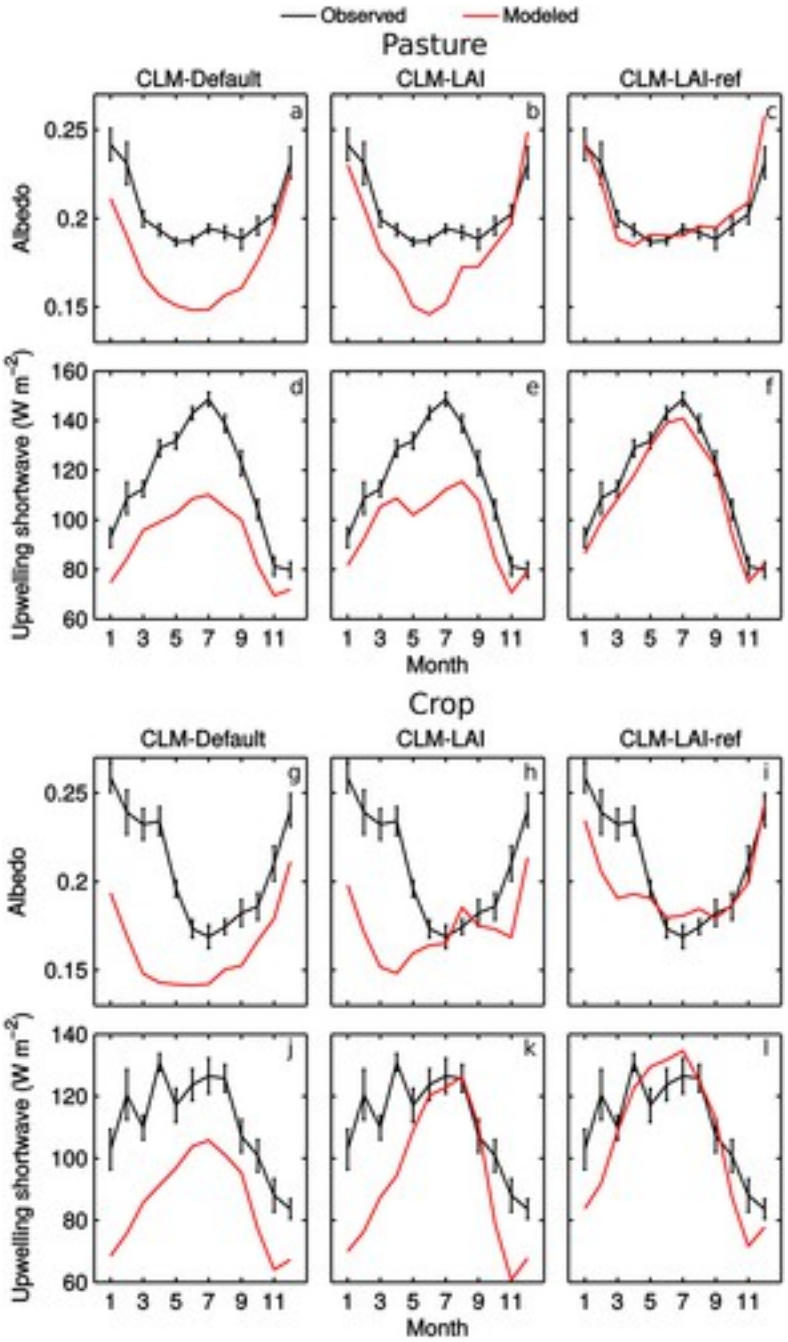

Figure 2

Open in figure viewerPowerPoint

Comparison of observed (black) and predicted (red) surface albedo for (a) default CLM, (b) CLM with prescribed site-level LAI, and (c) prescribed LAI with modified leaf reflectance, for the pasture site. (d–f) As in Figures 2a–2c but for upwelling (reflected) surface shortwave radiation. (g–l) As in Figures 2a–2f but for the crop site. Error bars indicate standard error of the mean.

Caption

We found large discrepancies between the (default) modeled and observed relationships between soil moisture and EF and between LAI and EF, using daytime averages (10–16 h local time) of

all variables. For pasture (Figure 3a), the observed EF was only weakly correlated with upper layer soil moisture at 10 cm depth (R^2=0.20), whereas default CLM predicted a much stronger correlation (R^2=0.56; Figure 3b). Furthermore, there was a strong correlation of observed EF with observed LAI (R^2=0.70; Figure 3d), whereas default CLM predicted no correlation with LAI (Figure 3e). Similar results were obtained for comparisons between observations and default CLM at the crop site (Figures 3g, 3h, 3j, and 3k), despite large differences in soil moisture and flux measurement methodologies between the crop and pasture sites. Therefore, the similarity between the correlations at the these two sites indicates that the results were not dependent on the choice of soil moisture or flux measurement methodology. These correlations suggest that CLM4.5 overestimates the influence of near-surface soil moisture and underestimates the influence of vegetation on EF, consistent with the analyses of *Swenson and Lawrence* [2014] and *Tang and Riley* [2013].

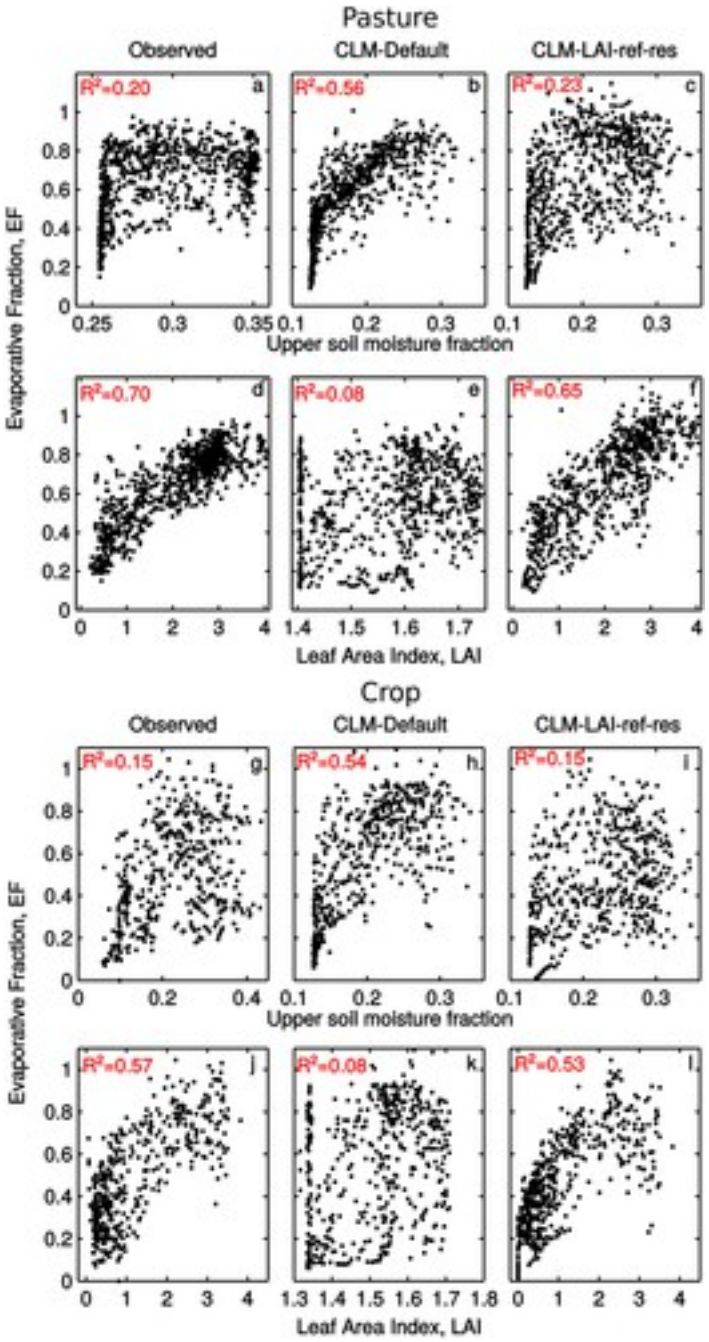

Figure 3

Open in figure viewerPowerPoint

Scatter diagrams showing relationships between soil moisture and evaporative fraction in (a) observations, (b) default CLM, and (c) CLM-LAI-ref-res, for the pasture site, for warm season months. (d–f) As in Figures 3a–3c but for the relationship between leaf area index and evaporative fraction. (g–l) As in Figures 3a–3f but for the crop site. Each point is a daily daytime average (note the larger range in daily LAI compared to climatological monthly averages shown in Figure 1, due to interannual variability). Squared correlation coefficients are indicated in the upper left of each panel.

Caption

Although we did not remove the seasonal cycle, the correlation between LAI and EF does not simply reflect seasonal covariation with a third variable (e.g., net radiation). Prior work has shown that the two sites analyzed here (crop and pasture) exhibit differences in EF of about 0.4 in April and 0.6 in June, despite sharing almost identical atmospheric forcing due to their proximity [*Williams and Torn*, 2015]. In that study, these differences in EF were largely explained by differences in LAI between the fields, suggesting an intrinsic influence of vegetation state on EF. Similar results have been shown at other sites in terms of an observed sharp increase in ET and corresponding decrease in temperature following spring leaf out [e.g., *Betts*, 2011].

While prescribing the observed LAI substantially increased the modeled correlation between LAI and EF (to R^2=0.53), the correlation between soil moisture and EF remained relatively high (R^2=0.42), and the reduction in this correlation was smaller for the crop site (results not shown in Figure 3). From these results we conclude that LAI partly explains the discrepancies between the observed and modeled correlations with EF. The remaining discrepancies suggest that bare soil evaporation may be excessive under high soil moisture (at 10 cm depth), while transpiration may be too limited under low soil moisture, in CLM4.5. As discussed in section (2.6), we increased the minimum stomatal conductance, increased the dry litter-layer resistance, and decreased the soil beta factor and V_{cmax}. To simplify the presentation, we report the results where soil and stomatal resistances were changed together with leaf reflectance, V_{cmax}, and LAI (hereafter referred to as CLM-LAI-ref-res). As shown later in this section, these parameter changes increased the contribution of transpiration and decreased the contribution of soil evaporation to ET, leaving ET relatively unchanged.

The predicted soil moisture-EF and LAI-EF relationships were improved in CLM-LAI-ref-res, for both pasture (Figures 3c and 3f) and crops (Figures 3i and 3l). The scatter diagrams are summarized by their correlation coefficients (Figure 4), including the results for CLM with site-prescribed LAI only (CLM-LAI). The CLM-LAI-ref-res experiment resulted in stronger correlations between LAI and EF (R^2 = 0.65) and weaker correlations between soil moisture and EF (R^2 = 0.23), consistent with the observations. This result suggests that the overpredicted correlations between soil moisture and EF commonly seen in land surface models result from overpredicted soil evaporation and underpredicted transpiration.

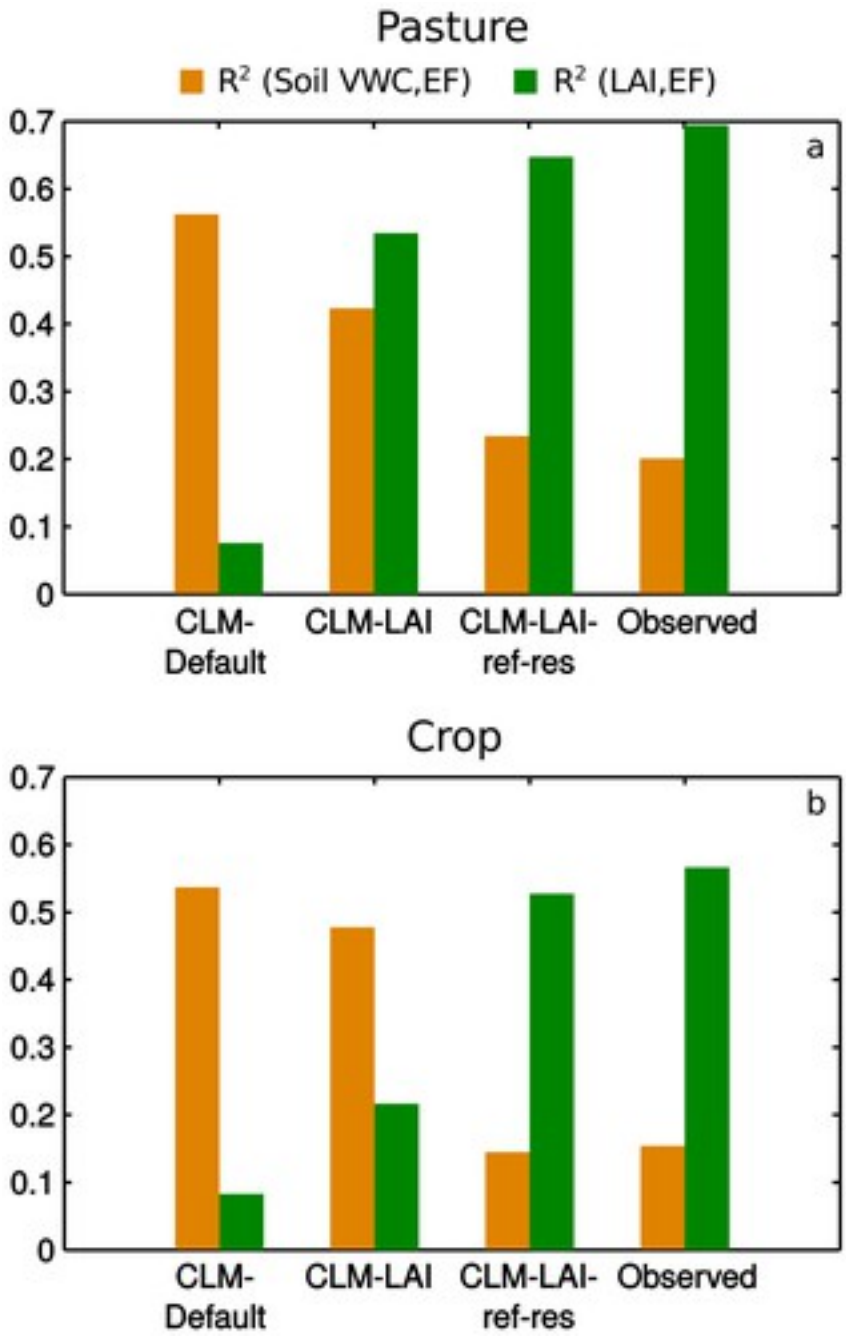

Figure 4

Open in figure viewerPowerPoint

Observed and modeled correlations between 10 cm soil moisture and evaporative fraction (orange), and between leaf area index and evaporative fraction (green), for (a) pasture and (b) crop fields.

Caption

In addition to correlation coefficients, we calculated the sensitivity index (hereafter *I*) for the relationship between soil moisture and EF [*Dirmeyer*, 2011]. We also estimated a sensitivity index for the relationship between LAI and EF (replacing soil moisture with LAI in the

definition of *I*). Table (2) summarizes results for the R^2 and *I* metrics, where we averaged the pasture and crop sites together to obtain single values for each metric (differences between the sites were relatively small and not shown). We found that *I* was higher for the relationship between LAI and EF than for the relationship between soil moisture and EF, indicating greater sensitivity of EF to LAI than to soil moisture. Default CLM underpredicted *I* for the relationship between LAI and EF. However, *I* was less sensitive than R^2 to differences between the modified versions of CLM.

Table 2. Observed and Modeled Terrestrial Coupling Metrics for the Relationship Between Soil Volumetric Water Content at 10 cm and Evaporative Fraction (VWC,EF) and the Relationship Between LAI and Evaporative Fraction (LAI,EF)

	Observation	CLM-default	CLM-LAI	CLM-LAI-ref	CLM-LAI-ref-res
I (VWC,EF)	0.13	0.16	0.15	0.16	0.15
I (LAI,EF)	0.30	0.04	0.27	0.29	0.30
R^2 (VWC,EF)	0.17	0.55	0.45	0.43	0.19
R^2 (LAI,EF)	0.62	0.08	0.38	0.41	0.59

We compared predicted and observed (24 h average) climatological monthly surface heat fluxes, to check that the preceding parameter changes improved prediction of the EF-LAI and EF-soil moisture relationships without degrading prediction of the surface fluxes themselves. In both the default and modified CLM runs, the different model configurations all showed a seasonal pattern of declining sensible heat flux and increasing latent heat flux in summer months when pasture LAI is highest (Figures 5a–5f), consistent with the expectation that latent heat flux would be higher during the peak growing season and would take energy away from sensible heat flux. This pattern was muted in default CLM (Figures 5a and 5d) and enhanced in the configurations with prescribed observed LAI (Figures 5b and 5c, and 5e and 5f). Default CLM underpredicted latent heat flux in summer months (Figure 5a). Both the CLM-LAI and CLM-LAI-ref-res configurations reduced the RMSE in JJA latent heat flux (see Table 3 and Figures 5b and 5c).

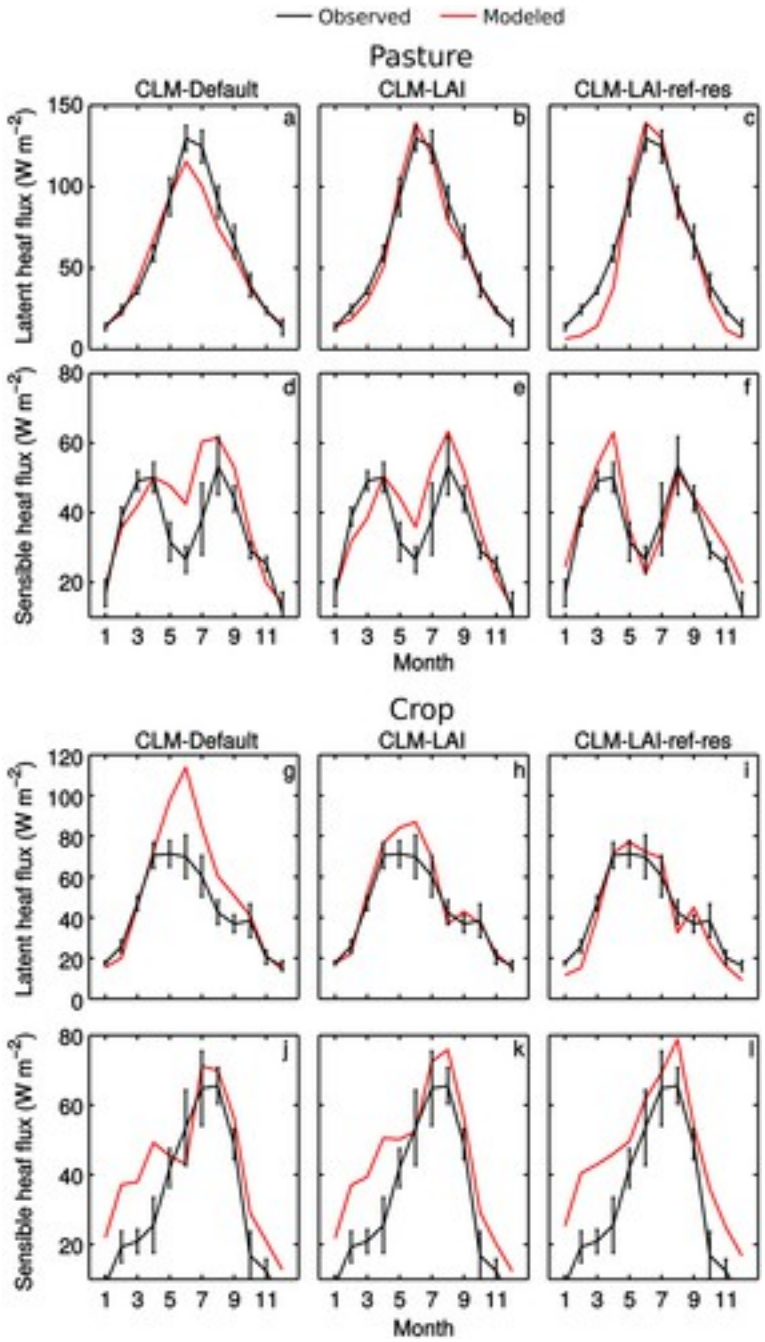

Figure 5

Open in figure viewerPowerPoint

Comparison of observed (black) and predicted (red) latent heat flux for (a) default CLM, (b) CLM-LAI, and (c) CLM-LAI-ref-res, for the pasture site. (d–f) As in Figures 5a–5c but for sensible heat flux. (g–l) As in Figures 5a–5f but for the crop site. Note the difference in *y* axis scale between sensible and latent heat flux. Error bars indicate the standard error of the monthly mean over multiple years.

Caption

Table 3. Bias and RMSE in JJA Monthly Latent (LH) and Sensible (SH) Heat Flux for the Pasture Site

	CLM-default	CLM-LAI	CLM-LAI-ref-res
LH flux bias (W m^{-2})	−15.83	−4.16	0.89
SH flux bias (W m^{-2})	11.69	9.41	0.82
LH RMSE (W m^{-2})	27.62	22.69	18.53
SH RMSE (W m^{-2})	21.65	15.99	11.47

Compared to the pasture site, the crop site showed larger improvements in monthly latent and sensible heat fluxes between the default and modified CLM configurations (Figures 5g–5l), related to the larger difference between default and observed LAI for crops compared to pasture. The crop field was typically bare or sparsely vegetated in early summer (June–July), and likewise its observed latent heat flux was significantly lower compared to the pasture site. In contrast, the crop latent heat flux in default CLM was very similar to that of pasture, consistent with nearly identical LAI between the crop and grass PFTs in default CLM at this site. It is common for crop fields in the SGP to have lower LAI than pasture fields in the summer months, as will be shown in the following section using MODIS observations.

Transpiration was 66% of ET in CLM-LAI-ref compared to 77% in CLM-LAI-ref-res, during May–August, averaged over crop and pasture PFTs (results not shown in figures). The differences were largest in August, when transpiration accounted for 56% in CLM-LAI-ref compared to 81% in CLM-LAI-ref-res. This increase in transpiration (in CLM-LAI-ref-res) is consistent with previous studies that indicate ET is transpiration dominated [*Jasechko et al.*, 2013] and that (default) CLM4.5 may underestimate the fraction of transpiration in ET [*Swenson and Lawrence*, 2014]. Although the parameter changes in CLM-LAI-ref-res degraded prediction of latent and sensible heat fluxes in winter months compared to CLM-LAI (particularly November–March; Figure 5), they reduced biases and RMSE in the predicted fluxes during summer months as shown in Table 3. This summertime improvement is sufficient for our purposes of exploring impacts of land model biases on summer climate prediction; however,

further work would be needed to develop new parameterizations capable of improving fluxes and terrestrial coupling across the annual cycle and at other sites [e.g., *Tang et al.*, 2015].

3.2 Single-Column CESM

We ran single-column CESM1.2.2 with the four different configurations of CLM4.5 described in section 3.1 and summarized in Table 1 (CESM-default, CESM-ref, CESM-LAI-ref, and CESM-LAI-ref-res). These configurations were the same as in the off-line land model simulations, except that we used 250 m resolution MODIS LAI averaged over the model grid cell (as described in section 2.3). The MODIS data was used in place of site-level LAI because it better represents the larger spatial scale of the coupled model grid cell (see section 2.3). The MODIS LAI (Figure 6) is qualitatively similar to the site-level LAI shown earlier and exhibits the same difference in LAI seasonality between crop and pasture. Since the default CLM4.5 LAI is derived from MODIS climatology, the total MODIS LAI in this study is almost identical to the default CLM4.5 LAI when averaged over all six summers for which we integrated the coupled model. However, the default CLM4.5 LAI does not adequately separate this (total) LAI into different PFTs, resulting in an underestimation of the differences in LAI seasonality between the crop and grass PFTs. Although these LAI differences tend to average out over the grid cell (i.e., pasture LAI is high when crop LAI is low, and vice versa), they can still influence climate because the surface fluxes are not linear functions of LAI [*Riley et al.*, 2009].

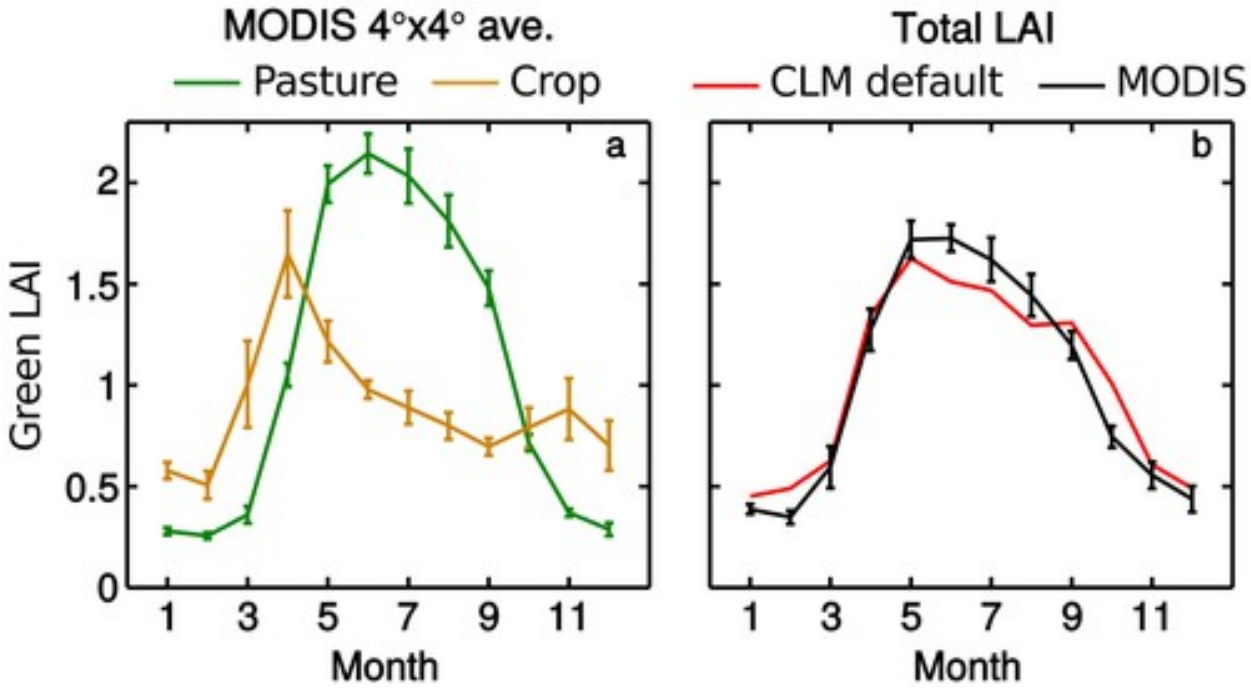

Figure 6
Open in figure viewerPowerPoint

MODIS LAI for the approximately 4° × 4° grid cell corresponding to the single-column model. (a) The 250 m resolution MODIS LAI separated into grass (green lines) and crop (weighted sum of LAI for summer and winter crop land use types) (orange lines). (b) Total LAI from default CLM (red) and MODIS (black), equivalent to the spatial average over all PFTs within the grid cell (i.e., the sum of LAI over all PFTs weighted by their fraction). Error bars indicate the standard error of the monthly mean.

Caption

We compared single-column CESM1.2.2 predictions to observations of temperature and total precipitation, for June, July, and August (JJA) (Figure 7). For temperature only, we show daytime-averaged (from 10 to 16 h local time) results in Figure 7. Biases in daily (24 h) temperature were qualitatively similar to those of daytime averages (not shown in Figure 7). Increasing the leaf reflectance (CESM-ref) reduced daytime temperatures (Figure 7a), and modifying LAI (CESM-LAI-ref) further reduced temperatures. Modifying the soil resistance and minimum stomatal conductance (CESM-LAI-ref-res) had a slight warming effect, with the exception of 2006. During the summer drought of 2006 [*Dong et al.*, 2011], a warm bias in daytime 2 m air temperature was reduced from +6°C to a smaller cold bias of −1.3°C, and a corresponding dry bias in total JJA precipitation was reduced from −111 mm to −23 mm (Figure 7b). A warm temperature bias was also significantly reduced in 2008, by nearly 4°C in the modified configurations, largely due to increased leaf reflectance. Biases in summer temperature prediction of similar or larger magnitude have been shown previously in CESM [*Lindvall et al.*, 2013] and other climate models [*Klein et al.*, 2006; *Merrifield and Xie*, 2016]. When considering all six summers simulated in the single-column model, the CESM-LAI-ref-res experiment reduced the root-mean-square error (RMSE) in daytime 2 m air temperature from 3.6 to 2°C in summer (JJA) and reduced RMSE in total JJA precipitation from 133 to 84 mm.

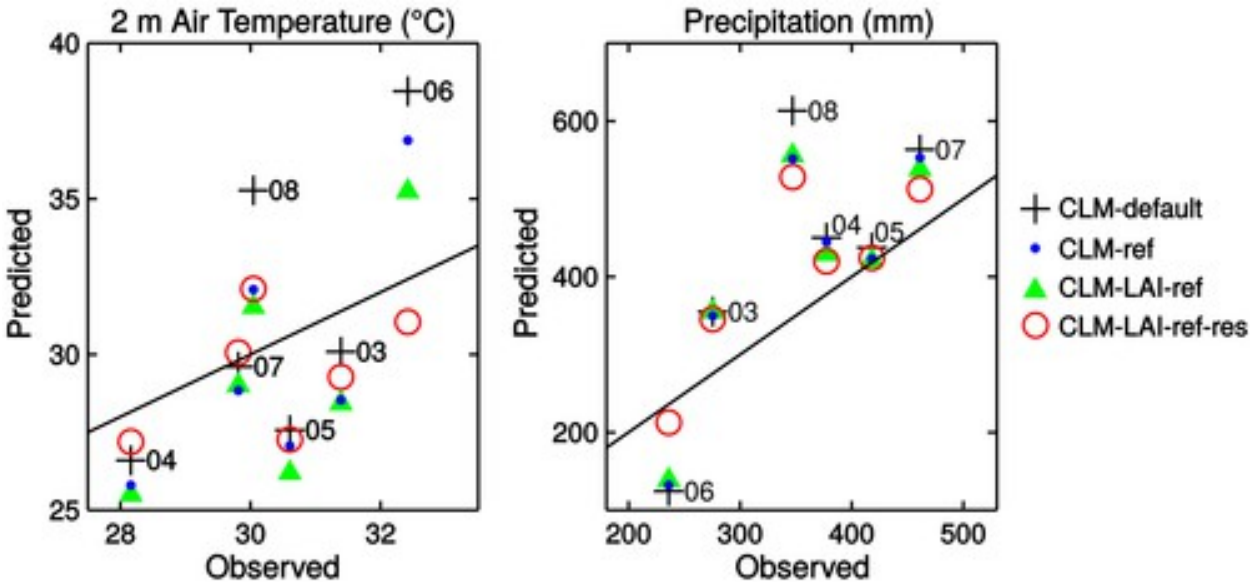

Figure 7

Open in figure viewerPowerPoint

Scatter diagram showing the relationship between observations and climate predictions over the grid cell of the single-column model. (a) Comparison of observed and predicted daytime 2 m surface air temperature, and (b) total (24 h) precipitation, for summer months (JJA). The year for each set of simulations is denoted by its last two digits. Solid black lines indicate 1:1 relationships.

Caption

In terms of the mean over all 6 years, CESM-LAI-ref-res made JJA climate drier by 18 mm. The default CESM had a wet bias of 72 mm during this period. For daily averaged temperature (not shown in Figure 7), the parameter changes in CESM-LAI-ref-res made the simulated JJA climate cooler by 1.4°C relative to the default. The default CESM had a warm bias in JJA daily averaged temperature of 1.8°C in daily averages.

The drought summer (2006) was the most sensitive to changes in the parameters controlling soil resistance and minimum stomatal conductance and was further analyzed to explore the mechanism underlying this sensitivity. The warm temperature bias began shortly after day 182 in CESM-default (Figure 8a) and coincided with a sharp decline in EF (Figure 8g). The default model underpredicted precipitation amounts per event and also failed to predict some of the precipitation events (Figure 8d). While the biases in temperature, precipitation, and EF were reduced in the CESM-LAI-ref configuration (Figures 8b, 8e, and 8h), the largest improvements came from modifying soil resistance and minimum stomatal conductance in CESM-LAI-ref-res (Figures 8c, 8f, and 8i). CESM-LAI-ref-res largely eliminated the dry bias and captured nearly all of the summer precipitation events (Figure 8f). Likewise, EF in CESM-LAI-ref-res increased and was more consistent with observations compared to the default CESM.

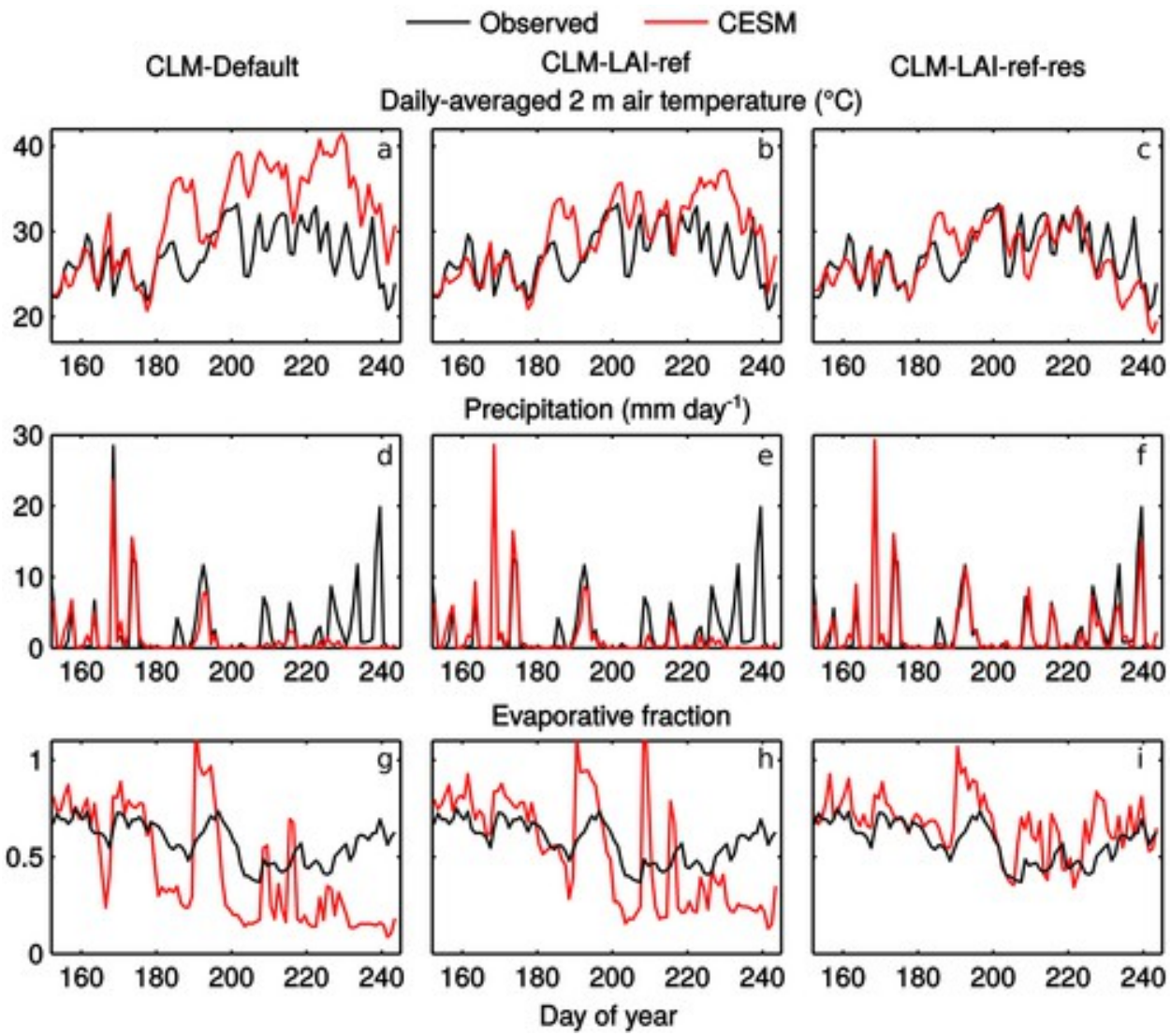

Figure 8

Open in figure viewerPowerPoint

Daily averaged 2 m air temperature for JJA of 2006, for the three CESM experiments having CLM configurations corresponding to (a) default CLM, (b) modified LAI and leaf reflectance, and (c) modified LAI, reflectance, stomatal conductance, and soil resistance. (d–f) As in Figures 8a–8c but for daily precipitation totals. (g–i) As in Figures 8a–8c but for daytime evaporative fraction.

Caption

Land surface variables were examined to determine the mechanisms by which modified soil resistance and minimum stomatal conductance reduced summer prediction biases in 2006. Although LAI was not substantially different between the default (Figure 9a) and modified configurations (Figures 9b and 9c), the predicted gross primary productivity (GPP), i.e., canopy-scale photosynthesis, was higher in the late summer (days 200–243) for CESM-LAI-ref-res (Figure 9c). CESM-LAI-ref-res also had higher latent heat flux from transpiration (green lines in

Figures 9d–9f). The soil latent heat flux (red lines in Figures 9d–9f) in late summer (days 220–243) was higher in CESM-LAI-ref-res, even though the soil resistance was higher. This higher soil evaporation was supported by enhanced upper layer soil moisture due to the higher precipitation amounts in CESM-LAI-ref-res, suggesting a positive feedback of soil moisture on precipitation.

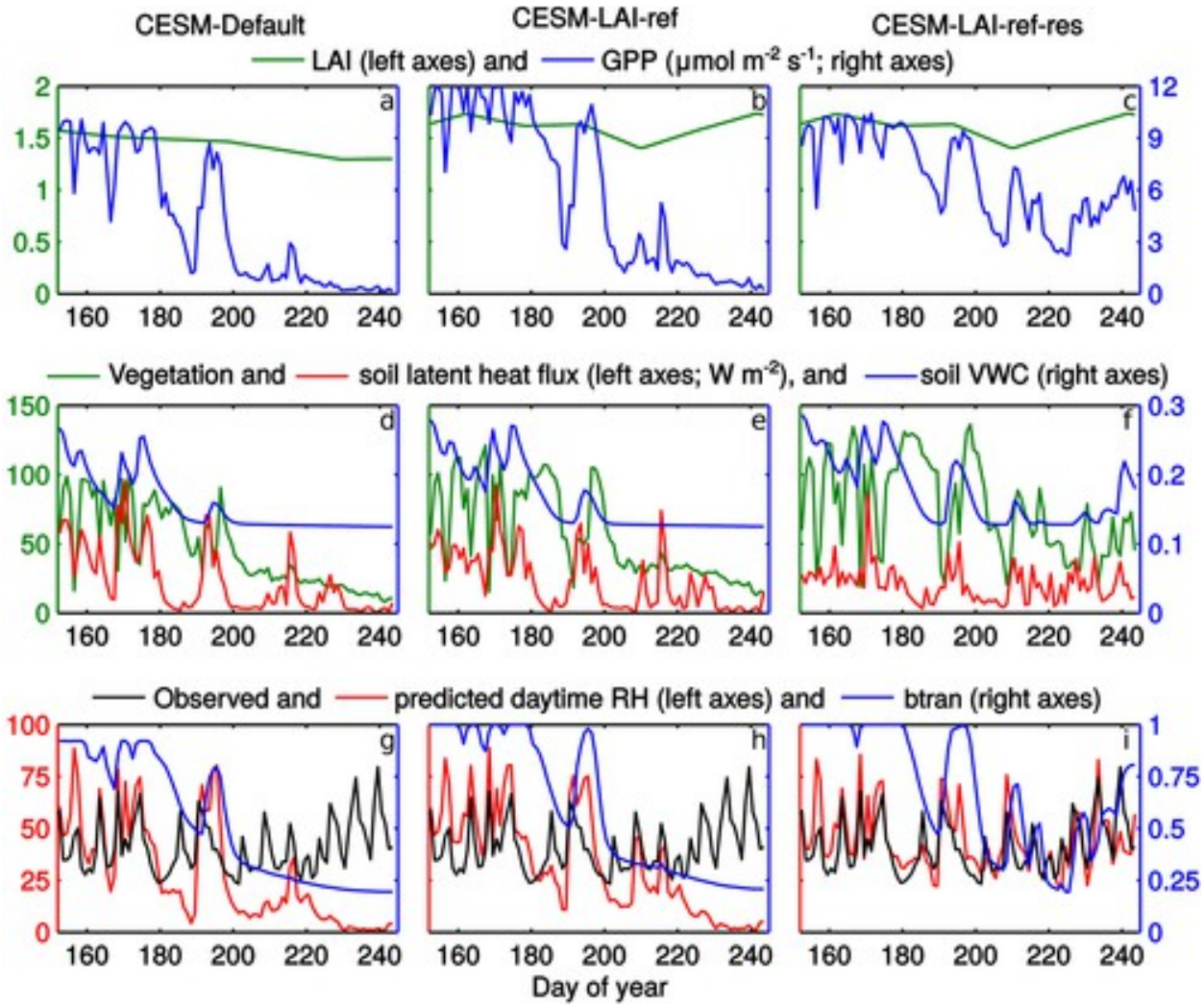

Figure 9

Open in figure viewerPowerPoint

As in Figure 8 but for land surface variables. (a–c) Leaf area index (green) and gross primary productivity (blue). (d–f) Vegetation transpiration (green) and soil (red) contributions to surface latent heat flux, and 10 cm soil volumetric water content (blue). (g–i) Observed (black) and predicted (red) daytime 2 m relative humidity, and soil moisture stress factor btran (blue).

Caption

The model representation of stomatal conductance depends on relative humidity and leaf turgor, which depends on soil moisture availability. The sharp decline in relative humidity starting near day 200 (Figures 9g–9i) is one reason for the decline in both GPP and transpiration, since both

GPP and stomatal conductance are positively and monotonically related to relative humidity [*Sellers et al.*, 1996]. In CLM4.5, GPP and stomatal conductance are also proportional to the soil moisture stress factor btran, which varies nonlinearly between 0 and 1 with soil moisture. Although btran sharply declined during the summer and thus contributed to the decline in GPP and stomatal conductance, it did not drop to 0, implying that soil dryness alone was not sufficient to shut off transpiration in any of the experiments. Separate simulations in which the relative humidity in the stomatal conductance equation was held at 50% (results not shown) confirmed the role of relative humidity explaining the sharp decline in GPP and transpiration in the late summer. The prediction of relative humidity was significantly improved in CESM-LAI-ref-res compared to observations (Figure 9i), supporting the possibility of a feedback of stomatal conductance on relative humidity. This feedback was triggered by a net moisture sink in the column advective tendency (not shown). Large-scale transport of moisture away from the SGP region was also documented previously in an analysis of the meteorological factors contributing to the 2006 drought [*Dong et al.*, 2011]. These results suggest that vegetation can create a positive feedback of soil moisture on precipitation, particularly in a dry atmosphere when evapotranspiration is the primary supply of water vapor for precipitation.

The effects of land model parameters on predicted summer climate can be summarized in terms of the change in relative contributions of modeled soil evaporation and transpiration to ET. All years showed a decrease in soil evaporation and an increase in transpiration in CESM-LAI-ref-res relative to the default CESM (Figure 10). However, the contributions of soil evaporation and transpiration were very different depending on the simulated year (Figure 10). In drier years (particularly 2006), transpiration increased much more than soil evaporation decreased, leading to a net increase in ET of sufficient magnitude to correct for the bias in ET seen in default CESM. In wetter years (particularly 2008), soil evaporation decreased more than transpiration increased, leading to a net decrease in ET. Years where ET was already well predicted by default CESM showed changes in soil evaporation and transpiration that tended to cancel, leaving ET relatively unchanged. A limitation of this analysis is the lack of direct observations of transpiration and soil evaporation, which would be useful in evaluating our modified land model configuration in terms of mean fluxes.

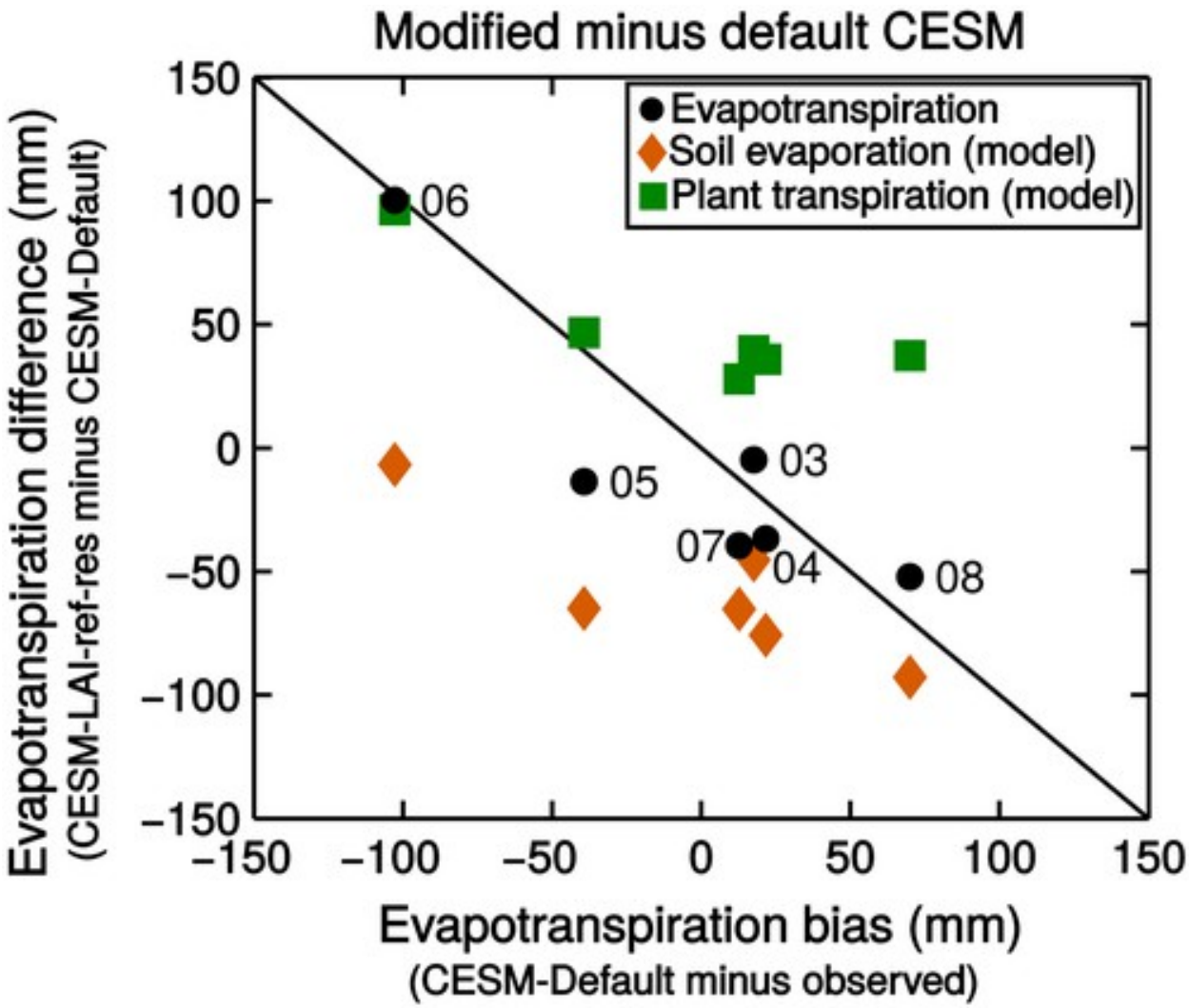

Figure 10

Open in figure viewerPowerPoint

Difference in ET (black circles) between modified (CESM-LAI-ref-res) and default CESM, shown as a function of the default model bias (difference between default CESM and observed ET). The black line indicates the difference in ET between modified and default CESM that would be required for a perfect prediction of ET in CESM-LAI-ref-res. The year for each set of simulations is denoted by its last two digits. Contributions of modeled transpiration and soil evaporation to the total change in ET are shown in green and orange. Relative to default CESM, CESM-LAI-ref-res increased transpiration more than it decreased soil evaporation at times when default CESM had too little ET (year 2006), and conversely when default CESM had too much ET (year 2008). Canopy evaporation of intercepted rainfall was a smaller component of summer ET at this site and is not shown.

Caption

We tested the sensitivity of our results to atmospheric initial conditions, by initializing the coupled model starting at 00:00 UTC on 1 July, 15 July, and 1 August 2006, using the same land surface initial conditions taken from the coupled model with the 1 June initialization. The different atmospheric initial conditions resulted in similar sensitivities of August temperature and

precipitation to land surface parameters (Figure 11). The relatively rapid onset of warm temperature biases for the 1 July and 1 August initializations (Figure 11a) is consistent with rapid onset of summer warm temperature biases shown in global climate models [*Phillips et al.*, 2004; *Klein et al.*, 2006; *Ma et al.*, 2014]. Here, the temperature bias develops by the end of the first day (in hourly output, not shown), leading to biases in the daytime-averaged temperature on the first day of the simulations for 1 July and 1 August shown in Figure 11a. The biases were significantly reduced in the integration with modified land surface parameters (Figure 11b). The sensitivity to land surface parameters is not a result of different soil moisture initial conditions, since all of the simulations (in Figure 11) shared the same soil moisture initial condition per initialization date. Using the spun-up off-line land surface initial conditions gave similar results, and the results were also not sensitive to initializing at 12:00 UTC (not shown).

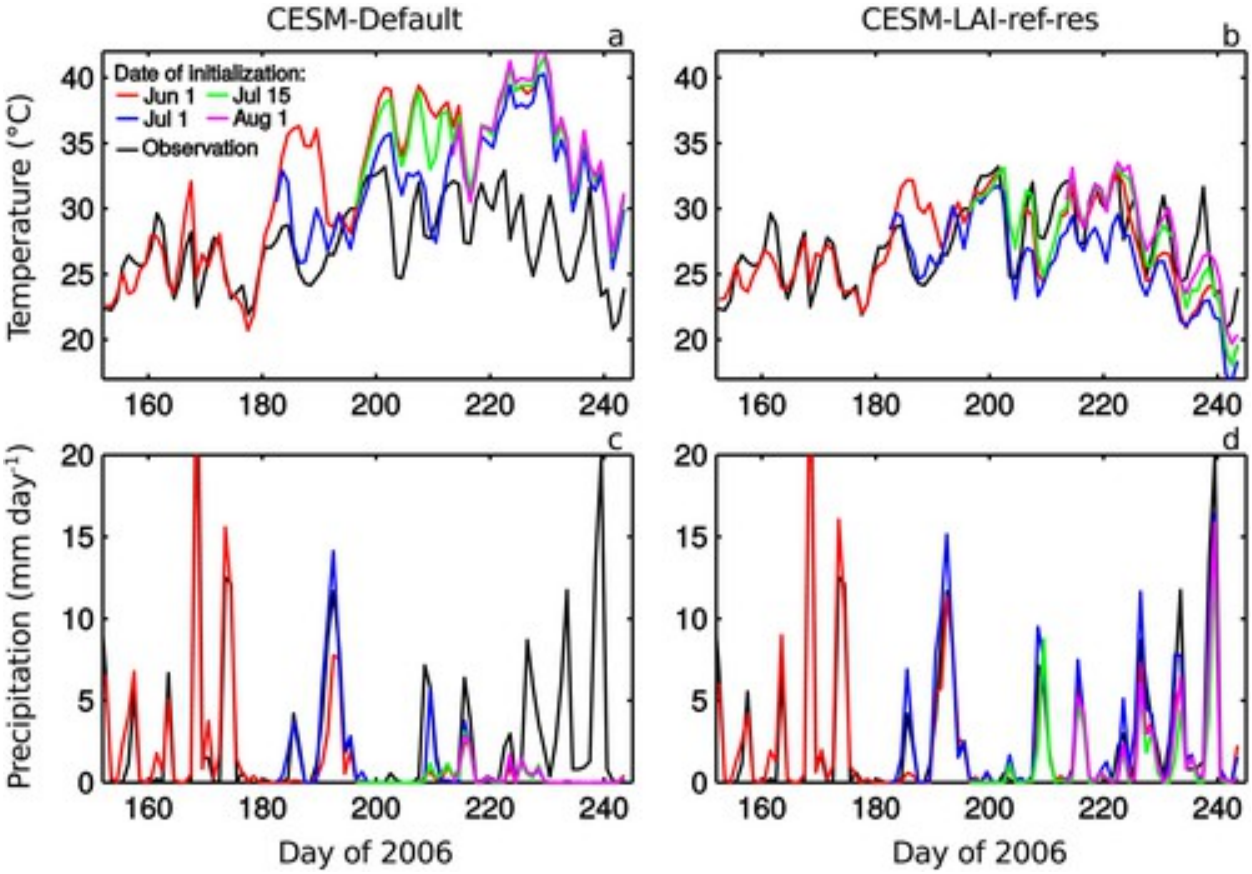

Figure 11

Open in figure viewerPowerPoint

Sensitivity to atmospheric initial condition. Daytime 2 m air temperature for JJA of 2006, for four different atmospheric initialization times, and for CLM configurations corresponding to (a) default CLM and (b) modified LAI, reflectance, stomatal conductance, and soil resistance. (c–d) As in Figures 11a and 11b but for daily precipitation totals. All initialization times result in similar predictions in August (days 213–243).

Caption

4 Discussion and Conclusions

Summer climate prediction is significantly influenced by the representation of land surface forcing in a single-column version of CESM1.2.2, shown here. Seasonal climate extremes were affected by the partitioning of ET into soil evaporation and transpiration, and by how this partitioning changes in wet and dry summers. The combination of increasing the soil resistance to evaporation and increasing the minimum stomatal conductance greatly improved modeled land-atmosphere coupling and had a positive impact on summer climate prediction. These land model modifications resulted in increased precipitation in dry summers and reduced precipitation in wetter summers. Additional work would be needed to determine if similar parameter changes can be applied more generally in other ecosystems and climates and to explore new land model parameterizations that may improve the predicted relationship between surface energy partitioning and land surface state. Our results may be relevant to other climates and ecosystems outside of the Southern Great Plains (SGP), particularly at times with low surface relative humidity, and considering that semiarid grasslands and humid continental deciduous forests were found to exhibit similarly strong relationship between LAI and EF as in the SGP [*Williams and Torn*, 2015].

Our results were not qualitatively dependent on soil moisture measurement depth. For example, the correlation coefficient between EF and soil moisture increased from R^2=0.21 at 10 cm depth to R^2=0.27 at 30 cm and R^2=0.31 at 60 cm, for the pasture site (as shown in *Williams and Torn* [2015]). While the correlation between 60 cm soil moisture and EF was greater than that between 10 cm soil moisture and EF, it was still weaker than that between LAI and EF. The relatively weak depth dependence of the soil moisture-EF correlations suggests the importance of considering soil moisture integrated over a plant rooting volume as opposed to values at single levels. Our results do not necessarily imply that LAI itself is not in part dependent on soil moisture. Rather, soil moisture stress and its effects on EF are complex functions of soil moisture, including its depth dependence and integration over time [*Williams and Torn*, 2015]. Vegetation state shapes this functional relationship, which is determined by coupling between soil physics and plant hydraulics [e.g., *Siqueira et al.*, 2008]. Additionally, soil moisture may be more of a driver of EF variability than LAI on shorter, daily timescales, since LAI is typically more slowly varying than (root-zone) soil moisture. The role of vegetation on such time scales could be assessed using gross primary productivity (GPP), which is expected to have a larger response to daily variability in soil moisture and atmospheric state than LAI.

The effects of vegetation described here help explain why modeled coupling between soil moisture and evaporative fraction is too strong in the SGP and other hot spot regions having strong modeled land-atmosphere coupling [*Ferguson et al.*, 2012; *Phillips and Klein*, 2014]. Consistent with those studies, we found that modeled soil moisture was too strongly correlated with EF in default CLM4.5. However, we also found that vegetation LAI was too weakly correlated with EF. Increasing modeled resistance to soil evaporation and increasing the minimum stomatal conductance led to weaker modeled correlations between soil moisture and EF, and stronger correlations between LAI and EF, in better agreement with observations. Apparently, CLM4.5 overestimates the influence of near-surface soil moisture and underestimates the influence of vegetation on surface energy partitioning. Additionally, the existing default LAI data sets do not adequately represent differences in LAI seasonality between crops and grasses. Overall, our results suggest that land-atmosphere coupling is not necessarily too strong in climate models but that the mechanisms of coupling are not adequately represented in land surface models. Whether the SGP would still emerge as a relative hot spot for land-atmosphere coupling would require further investigation in a regional or global model that can accurately represent the vegetation controls on EF shown here.

Our results indicate that vegetation helps maintain a more stable summer climate than would exist if ET were primarily driven by soil evaporation. This moderating effect is governed by the ability of vegetation to extract soil moisture over a greater depth than is available for direct soil evaporation at times of depleted upper layer soil moisture. This result is also consistent with a previous climate model study showing reduced precipitation variability due to vegetation transpiration [*Lee et al.*, 2012]. An important question is if climate change could push root-zone soil moisture past a minimum threshold beyond which transpiration cannot be sustained, and if current models can accurately predict the effects of such thresholds on climate change. Our results for the summer drought of 2006 suggest that some models may fail to predict changes in regional climate that would result from vegetation water stress, because they underestimate the role of vegetation (and root-zone soil moisture) in maintaining relatively high summer precipitation in the present day climate. A caveat to this extrapolation is that the single-column modeling experiments performed here do not include possible interactions with large-scale atmospheric dynamics. Furthermore, it is unclear how the effects of vegetation on climate extremes shown here would work under a scenario of elevated CO_2 including CO_2fertilization effects. Previous work has shown sensitivity of climate extremes to land model parameterizations in global warming projections [*Fischer et al.*, 2011; *Kala et al.*, 2016].

Previous work [*Lawrence et al.*, 2007] also demonstrated effects on climate prediction from modifying the partitioning of ET (into soil evaporation, transpiration, and canopy evaporation) in a previous version of CLM. There, the contribution of transpiration was increased by increasing root-zone soil moisture, and this had qualitatively similar effects on summer climate as found here. However, while those modifications resulted in a net increase in summer precipitation over the SGP by nearly 1 mm d^{-1}, the modifications here resulted in higher precipitation only during an unusually dry summer. On the other hand, the degree of coupling between soil moisture and EF was significantly reduced in the present study but remained strong under the modifications in *Lawrence et al.* [2007]. Our results for the summer drought of 2006 suggest that stomatal conductance may be too sensitive to low relative humidity in the default CLM and may lead to overpredicted reductions in transpiration in response to a dry atmosphere.

Our focus on column physics is a first step in studying land-atmosphere coupling, as the effects of atmospheric circulation feedbacks are mediated by the thermodynamic influence of the land surface on the PBL and overlying free troposphere [*Santanello et al.*, 2011]. The single-column approach has been used extensively for testing and improving clouds and precipitation in climate models [*Xie et al.*, 2004; *Hohenegger and Bretherton*, 2011]. Future work using global climate models would be needed to investigate possible interactions between the land surface and atmospheric circulation mediated by vegetation.

Leaf area index and soil moisture measurements provide complementary information on land-atmosphere coupling. Our results suggest that discrepancies in land-atmosphere coupling across different climate and land surface models may result from different model representations of vegetation controls on surface energy partitioning. A combination of soil moisture and vegetation-based observational metrics of land-atmosphere coupling would be helpful for improving modeled surface energy partitioning and evaluating its impacts on climate prediction.

Acknowledgments

Data for the SGP sites were obtained from arm.gov, from the following data streams: sgp30co2flx4mmetC1.b1 (http://dx.doi.org/10.5439/1025037), sgp30baebbrE13.c1 (http://dx.doi.org/10.5439/1027268), sgpswatsE13.b1 (http://dx.doi.org/10.5439/1150274), sgpmfrsrC1.b1 (http://dx.doi.org/10.5439/1023898), sgpmfrsrE13.b1 (http://dx.doi.org/10.5439/1023898), and sgp60varanarucC1.c1 (http://science.arm.gov/wg/cpm/scm/cont_index.html). This research used resources of the National Energy Research Scientific Computing Center, a DOE Office of Science User Facility supported by the Office of Science of the U.S. Department of Energy under contract DE-AC02-

05CH11231. This material is based upon work supported by the U.S. Department of Energy, Office of Science, Office of Biological and Environmental Research, Atmospheric System Research, and Atmospheric Radiation Measurement Programs, under contract DE-AC02-05CH11231. We thank Steve Klein, Tom Phillips, Hsi-Yen Ma, Yunyan Zhang, and Shaocheng Xie of Lawrence Livermore National Laboratory for helpful comments and suggestions, and for assistance in obtaining the variational analysis data.